Int. J. Radiation Oncology Biol. Phys., Vol. 59, No. 4, pp. 1217–1223, 2004

0360-3016/04/$–see front matter

doi:10.1016/j.ijrobp.2004.02.061

PHYSICS CONTRIBUTION

AN OPTIMIZATION ALGORITHM OF DOSE DISTRIBUTION USING ATTRACTION-REPULSION MODEL (APPLICATION TO LOW-DOSE-RATE INTERSTITIAL BRACHYTHERAPY)

Iori Sumida, M.Sc.,* Hiroya Shiomi, M.D.,* Ryoong-Jin Oh, M.D.,* Eiichi Tanaka, M.D.,† Humiaki Isohashi, M.D.,* Takehiro Inoue, M.D.,* and Toshihiko Inoue, M.D.*

*Division of Multidisciplinary Radiotherapy and †Department of Radiology, Osaka University Graduate School of Medicine, Suita, Osaka, Japan

Purpose: To optimize dose distribution for prostate cancer in low-dose-rate interstitial brachytherapy, we have developed a new algorithm named the Attraction-Repulsion Model. The purpose was to find the optimal source configuration.

Methods and Materials: The Attraction-Repulsion Model is used to optimize the dose distribution by finding the best seed configuration. We arranged grids at intervals of a certain space inside and established target and critical organs as areas of interest. We can make an attribute for grids, and the grids show attraction or repulsion depending on dose delivered from source. Source position is changed by the forces that the grids impose to the sources. A calculation was done repeatedly until the attraction and repulsion forces reached a balance. The optimal configuration was established when the sources reached a stable distribution in time. To evaluate the optimization plan, dose–volume histograms were used.

Results: Source configuration can be optimized automatically. The calculation time was approximately 5 min. The V100, V150, V200, and D90 of the target were 95%, 39%, 9%, and 157 Gy, respectively. V150 of the urethra and V80 of the rectum were 2% and 0%, respectively.

Conclusion: This method can optimize the dose distribution objectively. © 2004 Elsevier Inc.

Brachytherapy, Low-dose rate, Optimization, Attraction-Repulsion Model, Seed implant.

INTRODUCTION

During the last decade, radiation oncology has progressed with the multiplication of treatment modalities and techniques: three-dimensional (3D) conformal radiotherapy, radiosurgery, intensity modulated radiotherapy, and high-dose-rate (HDR) brachytherapy, have led to a new era of a computerized radiotherapy. With the availability of high-speed computers, calculation time of the dose distribution to a large number of volume elements is no longer a limiting factor.

A uniform dose throughout the target volume while sparing the normal tissues is often achieved with the help of optimization software, as in HDR brachytherapy. Various algorithms to optimize the dose distribution in HDR interstitial brachytherapy are suggested (*e.g.*, geometric optimization, dose point optimization) (1, 2). In a recent study, an anatomy-based dose optimization algorithm using fast simulated annealing algorithm was suggested (3, 4). In low-dose-rate (LDR) interstitial brachytherapy, Pouliot *et al.* described an optimization method of permanent ^{125}I prostate implants using fast simulated annealing (5). Yan *et al.* described a genetic algorithm for the optimization of prostate implants (6, 7). In general, the optimization problem in interstitial brachytherapy is to determine an optimal source configuration in permanent implant or to find the optimal dwell time distribution by changing dwell times in HDR brachytherapy, respectively.

In LDR interstitial brachytherapy, transrectal ultrasound-guided brachytherapy of the prostate is a major technique (8, 9). Our optimization objective is to determine the source configuration to the actual volume determined intraoperatively at the time of implantation.

The usual preplanning used to determine the optimal seed positions based on ultrasound images is suboptimal because of the differences in a patient's position or tumor shape occurring between the preplanning study and the implantation (10–12). Even if the seed were to be implanted at the optimal position according to the preplanning study, the seeds would not always be placed at the optimal position. In such a case, physicians have to adjust the optimal seed

Reprint requests to: Iori Sumida, M.Sc., Division of Multidisciplinary Radiotherapy, Osaka University Graduate School of Medicine (D10), 2-2 Yamada-oka Suita, Osaka 565–0871, Japan. Tel: (+81) 6-6879-3482; Fax: (+81) 6-6879-3489; E-mail: sumida@radonc.med.osaka-u.ac.jp

Received Apr 16, 2003, and in revised form Feb 20, 2004. Accepted for publication Feb 23, 2004.

position manually. Moreover, this approach is time-consuming and highly dependent on the skill and experience of the planner. For these reasons, we have devised a procedure consisting of a pretreatment optimization of the source placement associated with interactive planning during implant. The automation of preplanning that we propose here could save a significant amount of time to the planner, while increasing the reliability of the resulting dosimetry. Moreover, the radiation oncologist could, while trying to reproduce the preoptimized seeds positions, modify the plan according to each new situation occurring during the operative process.

We implemented a new method of optimization of sources placement using the Attraction-Repulsion Model derived from Gauss' law in electromagnetism. Our algorithm is based on the analogy between the arrangements of the sources in space, with the spatial configuration of charges inside a conductor until they reach electrostatic equilibrium. The objective function is analogous to the total potential of the electric field, whereas the sources positions are compared with the charge positions.

Our purpose in this article is to achieve the optimal dose distribution for LDR brachytherapy implant using the Attraction-Repulsion Model. After a brief description of the physics model, the relationship between clinical requirements and objective function is described. Results for a clinical prostate case with organs at risk is shown to illustrate the method.

METHODS AND MATERIALS

Attraction-Repulsion Model

The Attraction-Repulsion Model is based on Gauss' law, applying to a distribution of charges—all positive or all negative—in an electric field. The particles (charges) are first set randomly in space. Each is affected by the Coulomb forces that repel it from the surrounding ones. Every particle changes position until the electrostatic equilibrium is reached.

The Attraction-Repulsion Model that consists of six criteria:

1. Density of optimization grid points in the area of interest is uniform.
2. All optimization grid points have some attribution (attraction or repulsion).
3. Optimization grid points generate attraction or repulsion depending on dose or dose rate.
4. For each optimization grid point, attraction is defined as the force generated to increase dose or dose rate; repulsion is defined as the force generated to decrease dose or dose rate.
5. Both attraction and repulsion are determined as the function of dose or dose rate.
6. Optimization grid gives attraction or repulsion for one parameter of the source. For example, one parameter of the source is source position in permanent implant.

By analogy, we assumed in this study that the charges are radioactive point sources—emitting dose proportional to inverse square distance—and that the final distribution of charges is the dose distribution as required by the physician. For the optimization process that will lead us to the optimal source positioning, seeds were taken to be isotropic point sources. The dose calculation formalism incorporated the radial dose functions and the one-dimensional anisotropy factors recommended by the American Association of Physicists in Medicine Task Group 43 for ^{125}I seed sources (13).

In this study, we have used the Attraction-Repulsion Model to determine optimal source positions for brachytherapy seed implants of the prostate. The unit distance for optimization grid was 1 pixel and the pixel size was 0.33 mm. The size was calculated between the number of pixels, then grid interval of template was overlaid with the ultrasound image and the actual distance of grid interval. Any seed can move freely along the needle on the longitudinal axis, and any needle can move freely in the transverse plane. The minimum distance of movement for seed was 1 pixel.

Generation of optimization grid

Optimization of permanent prostate implants using the Attraction-Repulsion Model requires 3D information regarding prostatic shape, extent of local disease, and relative position of all dose-limiting normal tissue structures. A set of transverse images are acquired using transrectal ultrasound with the patient in the lithotomy position. A computer equipped with a frame grabber is connected directly to one of the video outputs of the ultrasound device. The first image is taken at the apex of the prostate and sequential images are taken at 5-mm intervals until the prostatic base is reached. The contours of prostate (target), urethra, and rectum (critical organs) were drawn by the radiation oncologist on captured images. A grid was generated with optimization points uniformly placed at a distance of 3 pixels (1 mm). Several hundred points were thus distributed into each contour. The optimization points also covered an area of normal tissues around the target (Fig. 1). The total area of optimization consisted of 240×240 pixels, and the number of slices were 15.

Each optimization point was defined by its position and its belonging to one or another of the four clinical structures. Depending on the prescribed dose to the organ it belongs to, each point was attributed different parameters of attraction or repulsion.

Definition of attraction and repulsion

For each optimization grid point, attraction was defined as the force that was generated to increase dose or dose rate, and repulsion as the force that was generated to decrease dose or dose rate.

Attraction and repulsion parameters setting

The clinical dose constraints were:

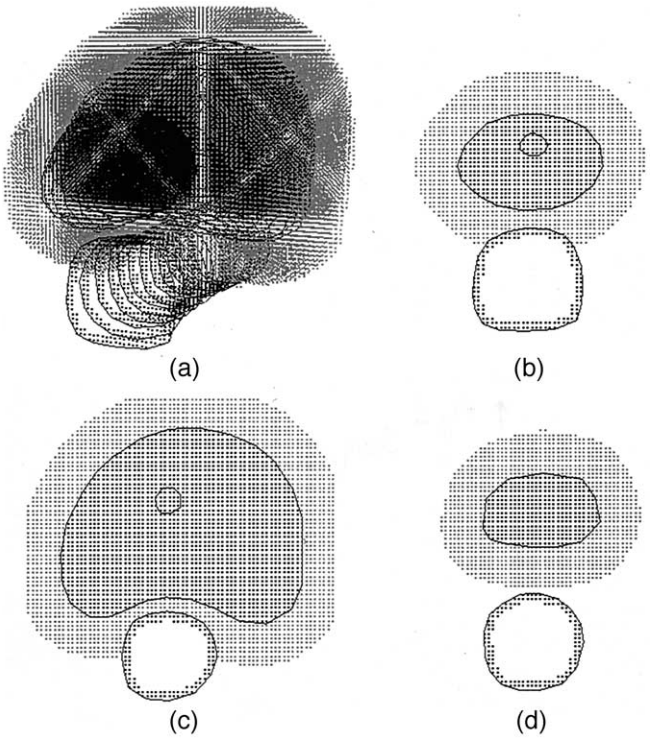

Fig. 1. Contour of prostate, urethra, and rectum, which a physician surrounded by manual labor and optimization grids (a). Grids shown in black were generated inside each contour; grids shown in gray were generated outside the contour of prostate. The apex (a), the axial midplane (b), and the base (c) of the prostate are shown in two dimensions.

- the dose to the prostate should be within a predefined dose range (minimum and maximum doses) called "target;"
- the dose to the urethra should be within a predefined dose range (minimum and maximum doses) called "urethra;"
- the dose to the rectum should not exceed the threshold dose called "rectum."
- the dose to normal tissues around the target should not exceed the threshold dose called "normal tissue."

Concretely, the attraction was defined as the force attracting the sources to the optimization point. Repulsion was the repelling force. Therefore, when the dose to a point of the target, or the dose to a point of the critical organs, exceeded the constraint, the optimization attributed repulsion to the point. When the dose at a point in the target was lower than the minimum dose constraint, then attraction was generated. Attraction was used for target coverage, whereas repulsion concerned maximum dose constraints to target and critical structures.

Initial position of needles and seeds

The clinical prostate case began with 14 needles. These needles were positioned at random in the axial midplane of the prostate to initialize the optimization process. The initial seed positions were distributed along each needle at 5-mm intervals from the base to the apex. These seeds have the alternative potential of the seed being active when it is located inside of the prostate contours and being passive when it is located outside the prostate contours. From these initial positions, the iterative algorithm decided of the next and following placements based on attraction-repulsion to the grid points and the value of the objective function.

Dose calculation to grid points

At each iteration, the seeds positions are known and their dose contribution to each optimization point can be calculated. In our study, we defined the dose-rate d_{ij} at a point i of the grid in relation to the source j. The expression of d_{ij} is according to (13):

$$d_{ij} = S_k \Lambda \phi_{an}(r_{ij})\, g(r_{ij})/r_{ij}^2, \tag{1}$$

where S_k is the air kerma strength, Λ the dose-rate constant, $\phi_{an}(r_{ij})$ the anisotropy function, $g(r_{ij})$ the radial dose function, and r_{ij} the distance between the source j and the grid i. From the dose-rate matrix d_{ij} obtained by Eq. 1, the calculation of the dose distribution D_i is given by the sum of the dose-rate contribution from all source positions j with a respective dwell time t_j:

$$D_i = \sum_j d_{ij} t_j. \tag{2}$$

However, in the case of permanent implants, the time is the same for all sources. Moreover, for this study, we have considered the distance from source to point as being the only factor affecting the dose.

Objective function

At each point i of the grid, the dose D_i (sum of the dose contributions of all sources j) must fulfill the clinical constraints. We have chosen a monomial expression for the objective function *f(i)*:

$$f(i) = \begin{cases} Gra_L \times (D_i - L) & \text{if } D_i < L \\ Gra_R \times (D_i - R) & \text{if } D_i > R \\ 0 & \text{if } L \le D_i \le R \end{cases} \tag{3}$$

where L is the minimum dose allowed to the target or critical organs, R is the maximum dose allowed to target or critical organs, and Gra_L and Gra_R are the slopes of the linear function *f(i)*. For the target, values of -40 and -8 for the gradients Gra_L and Gra_R were found to be a good parameter leading to the required dose distributions. When i belongs to the target, then, according to Eq. 3, and with the negative gradient, *f(i)* is positive if $D_i < L$, provoking attraction. *f(i)* is negative if $D_i > R$, then repulsion is generated. Figure 2 shows an example of objective function for a target. Basically, Gra_L is set to zero when i belongs to a critical organ. However, Gra_L was set to -40 when i belongs to the urethra, because the target coverage was increased resulting from attraction to the grid point. A

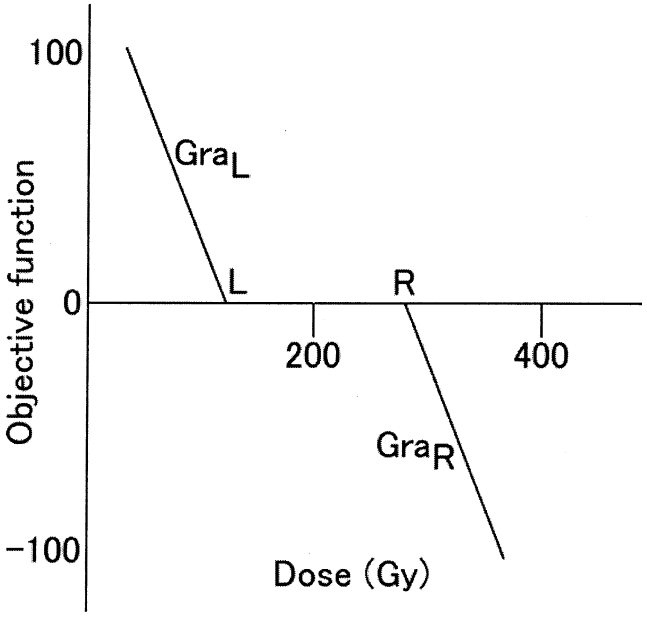

Fig. 2. Dose potential defined by Eq. (3).

negative gradient of −40 was also used for Gra_R. If $D_i > R$, then *f(i)* is negative and repulsion is generated. *f(i)* becomes zero when the dose to point *i* is within the clinical range. Figure 3 shows the objective function and parameters used for the clinical case and the four involved structures: target, urethra, rectum, and normal tissue.

At one step of the iterative process, for a given distribution of sources, the attraction or repulsion is implemented by the displacement vector $\hat{T}_j$:

$$\bar{T}_j = \sum_{i=1}^{n} f(i) \times \bar{U}_{ij}, \tag{4}$$

where $\hat{T}_j$ is the displacement vector for source *j*, *n* is the number of optimization grid points, and $\bar{U}_{ij}$ is the unit vector from point *i* to source *j*. The new source position must be restricted, because each source can move freely along the needle, but the source cannot move freely to transverse direction without the displacement of the other sources in the same needle. Therefore, the element of the new source position $\hat{T}_x new_j$, $\hat{T}_y new_j$, and $\hat{T}_z new_j$ are calculated by:

$$\bar{T}_x new_j = \bar{T}_x current_j + k \times \sum_{j=1}^{m} \bar{T}_{xj} \div m,$$

$$\bar{T}_y new_j = \bar{T}_y current_j + k \times \sum_{j=1}^{m} \bar{T}_{yj} \div m,$$

$$\bar{T}_z new_j = \bar{T}_z current_j + k \times \bar{T}_{zj}, \tag{5}$$

where $\hat{T}_x current_j$, $\hat{T}_y current_j$, and $\hat{T}_z current_j$ are the elements of the current source position, *k* is the gain parameter, and *m* is the number of active sources inside the needle. To avoid local minima, *k* was decreased gradually during the iterative calculation. In addition, a computer variable was implemented in the repulsion process, independent of dose, to avoid overlapping of sources. The new source configuration determined by Eqs. 4 and 5, is then used to start the next iteration.

Determination of optimal source positions

At the start of each iteration, the dose to the grid points was calculated. If the dose distribution to all points of the grid did not fulfill the requirements, then attraction and repulsion produced a new positioning of the sources. The sum of an absolute value of the objective function *f(i)* for each grid point *i* was used to stop the calculation. The process was repeated until the doses are all within the predefined constraints or the sum of an absolute value of the object function was not changed, which implies that the source positions remain unchanged. When the source placement reaches a point that is stable in time, then we assumed that it is the optimal solution.

Example of implant optimization

We tested our optimization algorithm with a clinical prostate case. The contours were drawn by a physician (Fig. 1). For a clinical prostate case, we have performed the optimization with 14 needles. Table 1 presents a set of parameters. Dose prescription was set to 145 Gy. To evaluate the implant optimization, the isodose distributions at each three slices for the apex, the axial midplane, and the base of the prostate were presented. Dose–volume histograms of the target and critical structures, the dose that covers 90% (D90) of the prostate volume, and the percentage of the prostate volume receiving 100% (V100), 150% (V150), and 200% (V200) of the prescribed dose were used (14, 15).

RESULTS

Clinical target with organs at risk

The dose distributions resulting from the optimizations with Table 1 are presented in Fig. 4. The 100% isodose distribution at the apex of the prostate did not completely encompass the target. The 100% isodose at the axial midplane of the prostate encompassed at least 95% of the target. The 100% isodose distribution at the base of the prostate did not completely encompass the target. In terms of the DVH of the target, V100, V150, and V200 of the target were 95%, 39%, and 9%, respectively. D90 was 157 Gy. At the axial midplane of the prostate, the urethra received less than 150% of the prescribed dose. The dose received by the rectum at any part of the prostate was less than 100% of the prescribed dose. In terms of the DVH of the critical organs, the urethra volume receiving 150% of the prescribed dose

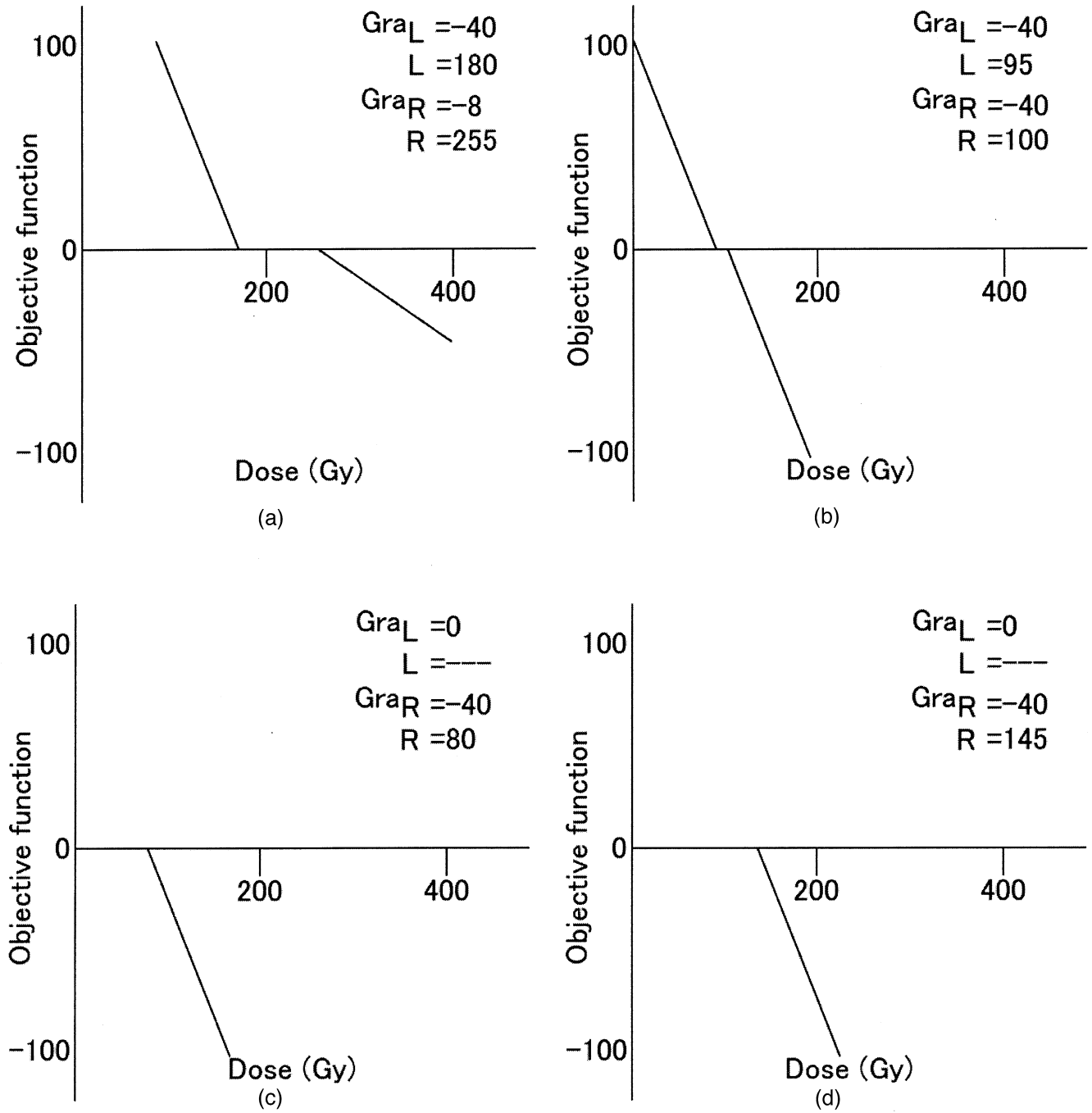

Fig. 3. Dose potentials chosen to satisfy the physician's prescription: (a) target-dose potential; (b) urethra-dose potential; (C) rectum-dose potential; and (d) normal tissue-dose potential.

was 2%. The rectum volume receiving 80% of the prescribed dose was 0% (Fig. 5).

Computational time

The computational time for the Attraction-Repulsion optimization of source positions and calculation of dose distributions depends on the number of grid points and the number of sources. For our case of 3D optimizations and the typical number of needles used, the running time on the Pentium III (1 GHz) was approximately 5 min.

DISCUSSION

The clinical objective in radiation oncology is to deliver a sufficient dose to the tumor while sparing the normal tissues. This is most difficult to achieve when organs at risk are close to the tumor. In brachytherapy prostate implants, the quality of

Table 1. Dose potential parameters of target and critical organs

	Gra_L	L	Gra_R	R
Target	–40	180	–8	255
Urethra	–40	95	–40	100
Rectum	0	—	–40	80
Normal tissue	0	—	–40	145

Prescribed dose: 145 Gy.

the implant often depends on the perception of the radiation oncologist and his or her ability to reproduce the preplanned treatment. Moreover, the preplanning process in which the planner tries to find the optimal source configuration by calculating a series of dose distributions is time-consuming.

The Attraction-Repulsion Model could be used to automate the optimization of seeds placement in an implant.

In the study of the clinical case, the dose distribution was also conformal with the dose protection of the urethra and rectum (Fig. 4). The majority of the target points received a dose 95%–100% of prescribed dose, except in the part of the apex and base. If each source can move freely in the optimization space, it is possible that the dose distribution will be higher conformally not only at the axial midplane but also at the apex and base of the prostate. However, movement of each source has limitation; therefore, it is in a needle. Moreover, it is not realistic to insert a needle whenever a source is inserted in the prostate. The sources at the apex and the base of the prostate have a tendency to concentrate, whereas those at the axial midplane of the prostate are more sparely distributed to fulfill the target coverage. With the maximum dose constraint of the urethra having been set with tighter constraint than that of the target, most points of the urethra receive less than 150% of the prescription. The volume of the urethra receiving 150% of the prescribed dose was 2%. The contour of the rectum was at a sufficient distance from the prostate, so that the volume of the rectum receiving 80% of the prescription was 0%. The constraints for normal tissue led to the high conformality of the target and also reduced the dose to rectal wall.

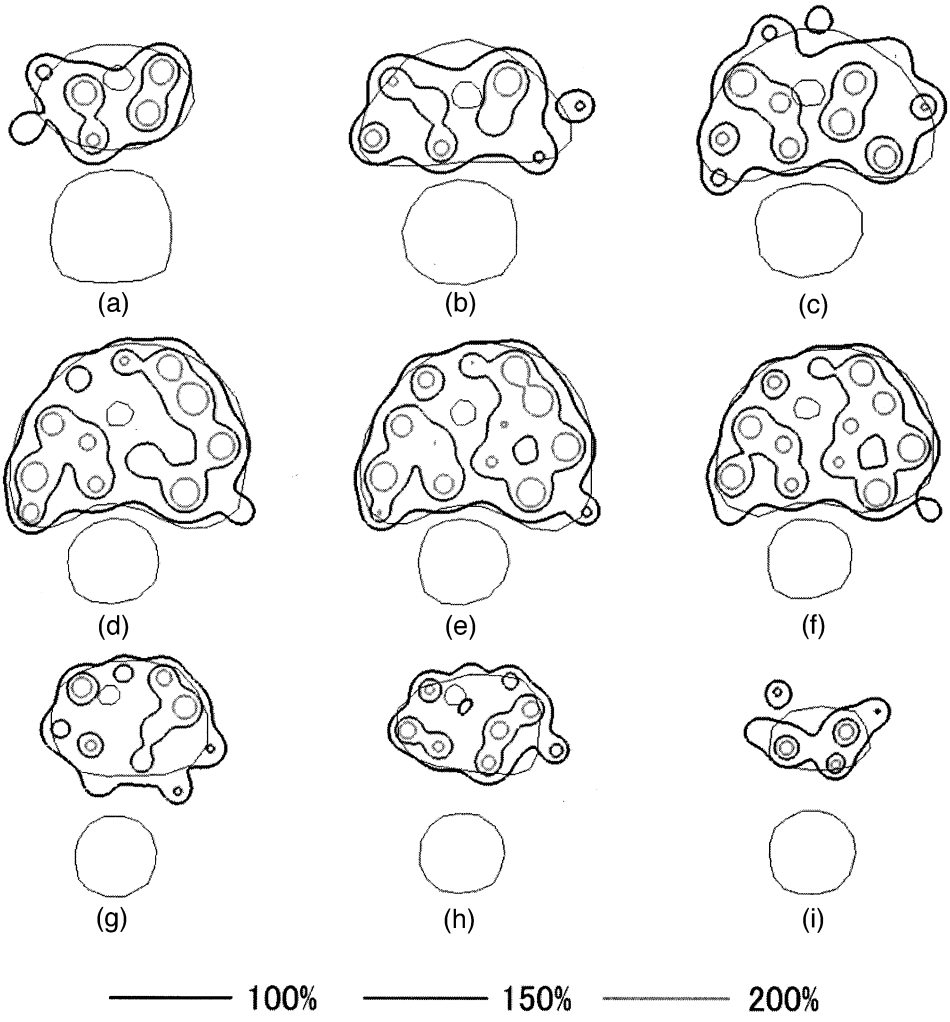

Fig. 4. Isodose distributions of each of three slices for the apex (a, b, c), the axial midplane (d, e, f), and the base (g, h, i) of the prostate obtained from clinical settings from Table 1. The isodose lines expressed are 1.0, 1.5, and 2.0 times the prescribed dose.

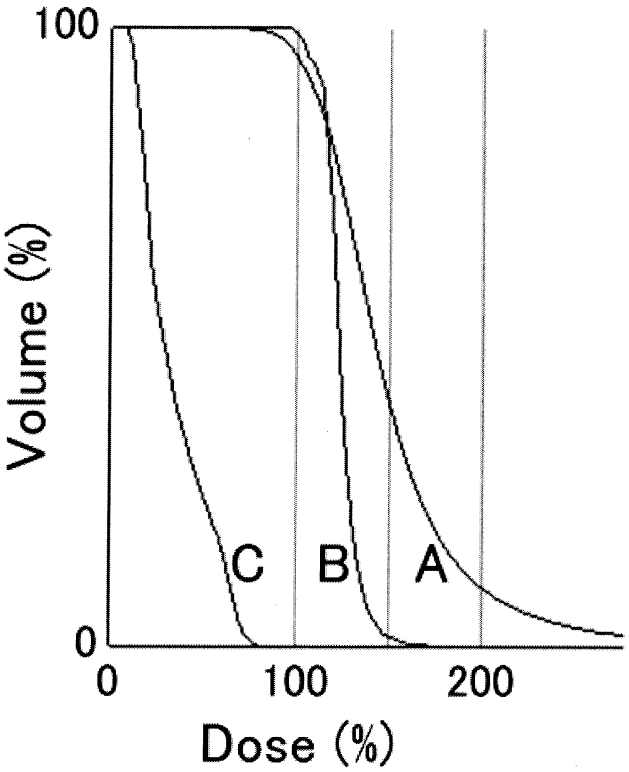

Fig. 5. Dose–volume histograms of the target (a), urethra (b), and rectal wall (c) of optimization plan.

In an actual treatment procedure for the permanent prostate implant, a needle template with 0.5-cm rectilinear grid spacing should be needed. Basically, the seed configuration space is defined as the set of all permitted seed positions. These potential seed positions are distributed along each needle at a certain constant intervals from the base to the apex. However, the optimization process using the Attraction-Repulsion Model didn't consider these situations; therefore, we will have to consider these situations to optimize the seed configuration in the next study.

CONCLUSION

By analogy with the charges configurations in a conductor after reaching the equilibrium state, the Attraction-Repulsion Model proves to be applicable to the problem of optimizing seed positions for brachytherapy implants, steering the optimization process to a rapid convergence. The computational time requires approximately 5 min to find the positions of many seeds in 3D optimization, because the computational time depends on a large number of grid points, seeds, and so on. The next step of our study will be to speed up the computational time and to implement an optimization procedure according to the actual treatment using the Attraction-Repulsion Model.

REFERENCES

1. Mould RF, Battermann JJ, Martinez AA, *et al.* Brachytherapy from radium to optimization. In: Laarse R, Prins TPE, editors. Introduction to HDR brachytherapy optimization. Veenendaal, The Netherlands: Nucletron Research B. V.; 1994. p. 331–351.
2. Edmundson GK, Rizzo NR, Teahan M, *et al.* Concurrent treatment planning for outpatient high dose rate prostate template implants. *Int J Radiat Oncol Biol Phys* 1993;27:1215–1223.
3. Lessard É, Pouliot J. Inverse planning anatomy-based dose optimization for HDR-brachytherapy of the prostate using fast simulated annealing algorithm and dedicated objective function. *Med Phys* 2001;28:773–779.
4. Lachance B, Béliveau-Nadeau D, Lessard É, *et al.* Early clinical experience with anatomy-based inverse planning dose optimization for high-dose-rate boost of the prostate. *Int J Radiat Oncol Biol Phys* 2002;54:86–100.
5. Pouliot J, Tremblay D, Roy J, *et al.* Optimization of permanent ^{125}I prostate implants using fast simulated annealing. *Int J Radiat Oncol Biol Phys* 1996;36:711–720.
6. Yu Y, Schell MC. A genetic algorithm for the optimization of prostate implants. *Med Phys* 1996;23:2085–2091.
7. Yu Y, Zhang JBY, Brasacchio RA, *et al.* Automated treatment planning engine for prostate seed implant brachytherapy. *Int J Radiat Oncol Biol Phys* 1999;43:647–652.
8. Holm HH, Pedersen JF, Hansen H, *et al.* Transperineal seed implantation in prostatic cancer guided by transrectal ultrasonography. *J Urol* 1983;130:283–286.
9. Blasko JC, Radge H, Schumacher D. Transperineal percutaneous iodine-125 implantation for prostatic carcinoma using transrectal ultrasound and template guidance. *Hypertherm Oncol* 1987;3:131–139.
10. Messing EM, Zhang JBY, Rubens DJ, *et al.* Intraoperative optimized inverse planning for prostate brachytherapy: Early experience. *Int J Radiat Oncol Biol Phys* 1999;44:801–808.
11. Yang G, Reinstein LE, Pai S, *et al.* A new genetic algorithm technique in optimization of permanent ^{125}I prostate implants. *Med Phys* 1998;25:2308–2315.
12. Beaulieu L, Aubin S, Taschereau R, *et al.* Dosimetric impact of the variation of the prostate volume and shape between pretreatment planning and treatment procedure. *Int J Radiat Oncol Biol Phys* 2002;53:215–221.
13. Nath R, Anderson LL, Luxton G, *et al.* Dosimetry of interstitial brachytherapy sources: Recommendations of the AAPM Radiation Therapy Committee Task Group No. 43. *Med Phys* 1995;22:209–234.
14. Nag S, Beyer D, Friedland J, *et al.* American brachytherapy society (ABS) recommendations for transperineal permanent brachytherapy of prostate cancer. *Int J Radiat Oncol Biol Phys* 1999;44:789–799.
15. Nag S, Bice W, DeWyngaert K, *et al.* The American brachytherapy society recommendations for permanent prostate brachytherapy postimplant dosimetric analysis. *Int J Radiat Oncol Biol Phys* 2000;46:221–230.